

We are IntechOpen, the world's leading publisher of Open Access books Built by scientists, for scientists

6,900

Open access books available

186,000

International authors and editors

200M

Downloads

Our authors are among the

154

Countries delivered to

TOP 1%

most cited scientists

12.2%

Contributors from top 500 universities



WEB OF SCIENCE™

Selection of our books indexed in the Book Citation Index
in Web of Science™ Core Collection (BKCI)

Interested in publishing with us?
Contact book.department@intechopen.com

Numbers displayed above are based on latest data collected.
For more information visit www.intechopen.com



Photocatalytic Treatment of Pesticides Using TiO_2 Doped with Rare Earth

*Juan C. Arévalo Pérez, José Gilberto Torres Torres,
Durvel de la Cruz Romero, Hermicenda Perez-Vidal,
Maria Antonia Lunagomez Rocha, Ignacio Cuauhtémoc López,
Adrian Cervantes Uribe and Zenaida Guerra Que*

Abstract

Rare earth doping ions can improve the spectral response of this semiconductor to the visible region. This work evaluated the dopant effect of rare earth ions such as La, Ce, Nd, Pr, Sm, Eu, and Gd in titania for the solar photodegradation of Diuron and methyl parathion. The increase in the content up to 0.5% of dopants decreases photoactivity due to the formation of photo-generated electron-hole pair recombination centers. The catalysts calcined at 500°C presented only the anatase crystalline phase and the samples doped with La and Ce at 0.1 and 0.3% were the most active in diuron solar degradation; however, when the temperature of the thermal treatment increased to 800°C , mixtures of crystalline phases were presented. The catalyst with the highest anatase content showed the best performance. The materials calcined at 500°C with better performance in diuron solar degradation were selected to treat methyl parathion using solar light. Finally, under these conditions, an affinity was found for the dopant ions in titania and in the functional groups of the contaminating molecules (phenylurea and thiophosphate). Solar photodegradation of diuron was more effective with La and Ce, while for methyl parathion, it was Eu at 0.3%.

Keywords: rare earth ions, doped TiO_2 , diuron, methyl parathion, sunlight

1. Introduction

Currently, the use of pesticides has increased in order to eliminate the pests that limit and reduce agricultural production in all countries of the world. Consequently, this has caused these substances to run off into natural aquatic bodies contaminating this medium. Diuron and methyl parathion have manifested this problem; hence, it is possible to find concentrations of these pesticides in aquatic bodies close to where they are applied [1]. Although the solubility in water is low, they can dissolve due to the surrounding environment. The presence of diuron and methyl parathion in water is difficult due to the persistence and stability they present [2].

In recent years, the elimination of these compounds in water has been reported by methods, physical [3], biological [4], and chemical [5]. Of the latter, advanced oxidation processes, such as heterogeneous photocatalysis, have been shown to be very efficient in the chemical transformation of pollutants up to their mineralization to CO_2 and other harmless compounds [6].

This process starts when a semiconductor is excited, with light that has a wavelength greater than or equal to the band energy of the semiconductor, to generate electron-hole pairs, which combine with the water and oxygen of the medium to form radicals that oxidize and mineralize the polluting organic matter [7]. TiO_2 is the ideal semiconductor used for this process; unfortunately, its spectral response is carried out at wavelengths corresponding to the UV region, which limits its use with natural sunlight because its spectrum only has a 5% UV light. Therefore, the investigations related to this semiconductor are made to improve its spectral response in the visible region, which has been achieved by doping the titania with different elements such as non-metals [8], transition metals [9], noble metals [10], and rare earth [11]. In this chapter, we analyzed the photocatalytic behavior under the natural sunlight of TiO_2 doped with La, Ce, Nd, Pr, Sm, Eu, and Gd at 0.1, 0.3, and 0.5% by weight thermally stabilized at 500 and 800°C for the degradation of diuron and methyl parathion.

1.1 Rare earth elements in photocatalysis

Rare earth ions have been used for doping TiO_2 aiming to modify the spectral response of the semiconductor to the visible light region to enhance its photocatalytic properties. Specifically, these ions can displace the phase transformation of anatase to rutile due to high temperature. Furthermore, have the capacity to form complexes with various base Lewis such as amines, aldehydes, carboxylic acids, alcohols, thiols etc., by the presence of electrons coming f-orbitals that interact with these functional groups, consequently allows in improving the absorptivity of organic pollutants in the aqueous medium and to elevate the photocatalytic activity [12]. These trivalent ions possess energy levels with a form of stair that as a dopant in a semiconductor can emit UV or visible light, through sequential absorptions from many near-infrared photons. The transformation of light from near-infrared and visible spectra toward UV range can be used to excite band gap of the titania [13].

On the other hand, luminescent properties of rare earth ions are originated by the electronic transition in the f-orbitals, which are partially full. These are sterically shielded from surrounding microenvironment by filled 5s and 5p orbitals, generating narrow bands with specific emission energy for each rare earth ion. This process provides properties unique to rare earth ions in photocatalytic applications [14].

At the end of the 1990s, the first investigations involving rare earth ions as dopants in TiO_2 for the photocatalytic oxidation were started [15]. Lin and Yu use a commercial photocatalyst (TiO_2 -P25) as a semiconductor for the acetone oxidation, doping this material with La. Then many reports appeared describing the doping of TiO_2 with rare earth ions applying methods of preparation such as solvothermal, microemulsion, impregnation, electrospinning, magnetron sputtering, and sol-gel [16]. The latter has been the most used due to its easy process and its low cost.

In previous studies, it has been found that the insertion of rare earth ions such as lanthanum in titania, cannot replace the position of Ti, due to the large size of the lanthanum ion with respect to Ti [17]. Typically, the rare earth ions on the surface of the TiO_2 are adsorbed in the form of oxides; only the titanium surface can be replaced by rare earth ions in the network of adsorbed lanthanide oxides, forming the Ti-O-L bond [18]. However, the substitution of a trivalent rare earth ion by a

tetravalent titanium ion creates an imbalance, favoring centers with positive charges, which could adsorb anions such as OH ions, to compensate the charge balance [19]. Therefore, the photo-generated holes can be consumed immediately after the load carriers are transferred to the surface, which increases the efficiency in the separation of charges. The photocatalytic benefits of the anatase and rutile phase in titania are widely known; the addition of rare earth ions in materials with these crystalline phases shows a growth in the crystal size, due to the presence of the Ti-O bonds, in the interface between TiO₂ and rare earth oxide formed [20]. In the interaction with anatase, the presence of these mentioned bonds inhibits the thermal transformation at the critical temperature of change, manifesting mixtures of crystalline phases at temperatures above 700°C in titania.

The rare earth oxides modified with titania show a growth in the intensity of light absorbed compared to pure TiO₂. According to Yan et al., incident photons can be scattered and lost by reflection on a smooth surface, while on a rough surface, formed by the presence of rare earth oxides, allows a large number of scattered photons penetrate the interior of the particle to activate the separation of charges [21].

In inorganic semiconductors such as TiO₂, light absorption is mainly attributed to the transition from the valence band to the conduction band, which is commonly referred to as band transitions. However, it is believed that, in the presence of lanthanide oxides, the increase in the intensity of light absorption is due to the transition of the electrons belonging to layer 4f of the lanthanides, known as the transition $f \rightarrow f$. The corresponding energy can be transferred to the titania to separate the charges [22].

1.2 Pesticides treated by photocatalysis

1.2.1 Diuron

Diuron (3-(3, 4-dichlorophenyl)-1, 1-dimethylurea) is a white, crystalline and odorless powder, which has low solubility in water (36.4 mg/L). Herbicide is employed for weed control in non-crop areas and to control weeds in a range of tree crops. Its mechanism of action mainly acts inhibiting photosynthesis by blocking electron transport at photosystem II [23]. When it is applied to soils, it is leached from 3 to 5 cm and strongly adsorbs persisting up to 330 days. In aqueous medium, it is partially absorbed due to its solubility, by the action of solar photolysis and OH radicals present in the environment, almost completely degraded, but this process is too slow and depends on environmental conditions [24]. For this reason, advanced oxidation processes such as heterogeneous photocatalysis with TiO₂ have been used to eliminate this herbicide as a water pollutant.

When TiO₂ is used as a colloidal particle in an aqueous solution of diuron, only one transformation is observed in the aliphatic chain, where the OH radicals attack the benzene ring causing its opening to aliphatic chains. In the presence of acetonitrile, the reaction mechanism indicates a reductive discoloration of the benzene ring, without it an oxidative demethylation of the aliphatic chain is observed [25].

The modification of TiO₂ with noble metals has improved the activity of this semiconductor for photodegradation and mineralization of diuron in an aqueous medium. Katsumata et al. impregnated the P25 at different doses of Pt in an oxidized state, stabilizing thermally up to 700°C. They described that 0.2% of Pt in TiO₂ showed the best performance in the photodegradation of diuron in a period of 20 min, and this material is four times more active than pure P25. Nevertheless, 97% of mineralization was reached after 8 h [26].

1.2.2 Methyl parathion

Methyl parathion (O, O-dimethyl O-p-nitrophenyl phosphorothioate) is a white crystalline powder that has a pungent smell like garlic and has low solubility in water (55 mg/L). As insecticide helps to control the biting and sucking of insects in fruit and vegetable crops, it is also applied in the fight against mites, Coleoptera, and caterpillars [27]. Furthermore, methyl parathion is capable to inhibit the action of acetylcholinesterase of nerve tissue, following its metabolic conversion to its corresponding phosphates methyl paraoxon and paraoxon. Organophosphate pesticides are generally regarded as safe for use on crops and animals due to their relatively fast biodegradation, but depend on microbial composition, pH, temperature, and sunlight. This compound can be degraded rapidly by hydrolysis in the presence of sunlight and air [28]. Physical, chemical, and biological methods have been used to minimize the toxic effect generated by this pollutant in water. One of the methods most used for this purpose is heterogeneous photocatalysis with titania, due to its high effectiveness to mineralize organic pollutants in an aqueous medium.

Many reports have been cited in the literature describing the photodegradation of the methyl parathion using TiO_2 with UV light under different conditions. Evgenidou et al. analyzed the photocatalytic behavior of TiO_2 and ZnO in the degradation of methyl parathion in an aqueous medium. They determined that the titania is more effective as a photocatalyst, presenting a higher reaction rate; in addition, this material could complete the mineralization process, without introducing unwanted intermediaries in the reaction [29].

On the other hand, investigations have been carried out involving the modification of TiO_2 to improve its photocatalytic behavior in the degradation of methyl parathion. Senthilnathan and Philip doped the titania with N using different precursors such as triethylamine, ethylamine, urea, and ammonium hydroxide. Their results show that the highest photoactivity is obtained using triethylamine, however, this catalyst when used under UV light did not show a higher performance than P25- TiO_2 , but when used with visible irradiation its effectiveness was the best [30].

1.3 TiO_2 doped with rare earth

Rare earth ions have been doped in TiO_2 as a strategy to increase the response of the semiconductor to the visible light region and enhance photocatalytic activity. It was reported in the literature that the optimum level of rare earth doping is less than 2% to hinder the crystal growth of titania during calcination [31]. Also, it is known that the rare earth ions occupy substitutional sites in the titania according to the analyzes carried out by XRD, but in many publications, this statement is contrary, due to the effect of the large ionic radionics of the rare earth ions, which they can only occupy interstitial sites or form aggregates such as oxides or hydroxide at the boundaries of the titania grain by creating Ti-O-RE bonds. The presence of this link generates an imbalance of charges with a positive charge center, which allows adsorbing anions to reach equilibrium. Therefore, the photo-generated holes can be consumed immediately after being transferred to the surface of the titania, whereby the separation of charges is improved; the process of recombination of hollow electron pairs is avoided, and consequently, the photocatalytic activity is favored [16]. Another effect, which inhibits the recombination process and therefore increases the photocatalytic yield of titania, is the formation of the Ti^{3+} species and the oxygen vacancies, both act as photo-generated hole capturers (valence band),

and together they are charged and at the same time, the oxygen of the medium traps the photo-generated electrons (conduction band); and this increases the separation of the photo-generated species. Ti^{3+} is oxidized in the presence of the oxygen present to generate the anion superoxide (O_2^-), which reacts with the photo-generated holes in order to produce hydroxyl radicals (OH^*) in an aqueous medium, and thus be able to oxidize any organic compound present in this system [6].

Rare earth dopant ions such as Pr, Ce, Nd, Eu, Sm, Dy, Gd, and La show significant enhancement in dye photodegradation compared with TiO_2 pure, due to the higher adsorption and the $4f$ electron transition of rare earth ions. Between 0.5 and 1% wt of doping ions, the best photocatalytic behavior of the doped samples are shown [31]. On the other hand, La, Nd, Sm, Eu, Gd, and Yb as dopants in TiO_2 , increase the titania yield and raise the stability of the anatase phase and prevent the segregation of titania. Likewise, these ions play a role in providing a means of concentrating the contaminants to be eliminated on the surface, and consequently, increasing the photocatalytic activity of semiconductor [32]. Recently, La, Nd, Eu, Sm, Gd, Er, Tb, Yb, Pr, and Ce when used as dopants improve the performance of titania, because it increases the absorption capacity of light, to surface and structural modifications, which has allowed the development of catalysts with environmental applications such as the degradation of pollutants in aqueous medium [33].

1.4 Methods of synthesis of $\text{TiO}_2\text{-RE}$

There are several methods used for the preparation of TiO_2 doped with rare earth ions, they exist from the most complex and expensive to the simplest and cheapest. These methods vary depending on the final structure that is desired, for example, to obtain thin films or coatings, the following methods are more used: Micro-arc oxidation [34], magnetron sputtering [35], spin coating [36] and dip coating [37]. To prepare powders with defined nanostructures are electrospinning (nanofibers) [38], anodization (nanotubes) [39], microemulsion (spheres) [40], hydrothermal (nanowires) [41], state solid reaction (amorphous) [42], impregnation (amorphous) [43], and sol-gel (different structures) [44]. All of them can be modified, combined with each other or coupled to different energy sources, such as microwaves [45] and ultrasounds [46], to create doped materials with unique photocatalytic properties.

1.4.1 Sol-gel

The sol-gel method has been the most used process for the synthesis of TiO_2 doped with rare earth ions due to the modifications that can make it, at its low cost and easy operation. With this method, crystalline titania can be prepared on a nanometric scale, with a high purity at low temperatures, stoichiometrically controlling the composition when dopants are inserted. This technique is also used for the synthesis of materials with spectral response in the visible region. In this process, the monomers in solution are hydrolyzed and polycondensed to form a polymer network in gel form (during this step, most of the authors report the insertion of doping ions), which contains a liquid phase and a solid phase. After the formation of the gel, the xerogel is formed by removing the solvents in the medium, and then thermal stability is provided by calcining the xerogel at temperatures above 200°C , until obtaining a dense solid with the desired crystalline structure [44].

1.4.2 Impregnation

Wet chemical impregnation is the very simple preparation method to implement to synthesize titania doped with rare earth ions; its process is very easy to perform; it employs mild working conditions and a low energy cost. It provides a uniform distribution of the dopant with the surface of the TiO_2 , generating an excellent adhesion between both, which allows controlling the structure, morphology, and particle size simply by modifying conditions such as rotation speed or agitation, contact time, system pH, and nature of solvents. This procedure can be summarized in three simple steps: (1) Place the titania in contact with an aqueous solution containing dissolved dopant precursors for a certain time in constant agitation. (2) Remove excess water in the system, and (3) Activate the material obtained with thermal treatments at elevated temperatures. The variables that mostly influence the preparation of titanium oxide doped with this method are listed below: morphology and structure of TiO_2 , amount of dopant material and its disposition with titania, types of solvents used, system pH and type of treatment thermal employed. Under the control of these conditions, this process allows being constantly reproducible [47].

2. Materials and methods

2.1 Characterization techniques of TiO_2 -RE

TiO_2 doped with rare earth ions were characterized by XRD, N_2 physisorption, Raman spectroscopy, scanning electron microscopy, and Uv-Vis spectroscopy with diffuse reflectance to describe the electronic, structural, and morphological properties.

2.1.1 UV-Vis (DRS)

UV-Vis spectra were used to estimate the band gap energy (E_g) for each catalyst, if the absorption coefficient (α) is zero, according to Eq. (1). This was performed in a UV-Vis spectrophotometer equipped with an integrating sphere for diffuse reflectance (Varian model Cary 300) using BaSO_4 as a reference [48].

$$\alpha(h\nu) = A(h\nu - E_g)^{\frac{m}{2}} \quad (1)$$

2.1.2 X-ray diffraction (XRD)

A Bruker model D8 advance X-ray diffractometer with anode of $\text{Cu K}\alpha$ radiation ($\lambda = 1.5418 \text{ \AA}$) was used. The samples were measured in the range of $2\theta = 20-70$ with a 0.02° step at a rate of 1 s/point at room temperature. To obtain the crystallographic planes of the crystal structures in the samples; they were identified through the library of the Joint Committee on Powder Diffraction Control Standards (JCPDS). The crystal size was calculated in nm (D) of the crystalline phases with the Scherrer Eq. (2) [48]:

$$D = \frac{K\lambda}{\beta \cos \theta} \quad (2)$$

The percentage of the Rutile phase (%R) was determined using Spurr Eq. (3) [49]:

$$R = \left(\frac{1}{1 + \left(0.8 * \frac{I_A}{I_R} \right)} \right) * 100 \quad (3)$$

2.1.3 BET surface area by N₂ physisorption

Micromeritics ASAP 2020 equipment was used to obtain the specific surface area and pore diameter distribution. Results were calculated from nitrogen adsorption isotherms. Before measuring, the samples were outgassed at 350°C for 2 h.

2.1.4 Raman spectroscopy

Spectra were obtained by a PerkinElmer Spectrum GX NIR-FT Raman spectrometer equipped with a microscope and CCD detector. Spectra were taken at room temperature and using a 5145°A line and argon ion laser (model spectra physics 2020) excited with of 50 mV of energy [50].

2.1.5 Scanning electron microscopy

A scanning electron microscope JEOL model JSM-6010LA was used to identify in detail the surface morphology of the photocatalysts. The analyzer X-Ray Energy Dispersive Spectrometry (XEDS) was used for elemental mapping in materials.

2.2 Synthesis of TiO₂ doped with Ce³⁺, Pr³⁺, La³⁺, Nd³⁺, Sm³⁺, Eu³⁺, and Gd³⁺

Rare earth doping was made using nitrate salts of each element. Water solutions of these salts were prepared to calculate the stoichiometric amount in order to obtain 0.5, 0.3, and 0.1 wt% according to the desired composition of the sample. A mixture of ethanol, water, and salt solution of rare earth was stirred and maintained under reflux at 70°C. Enough NH₄OH was added to the mixture to obtain pH 7. Titanium n-butoxide was added dropwise to this solution, stirring and refluxing was maintained for the period of 24 h until gel formation. The gels were dried in a rotating evaporator at 70°C under vacuum, subsequently, gels were placed into an oven at 120°C during 12 h. Samples were calcined at 500 and 800°C during 4 h with a heating ramp of 2°C/min. The same procedure was carried out but without adding the precursors of the rare earth ions to obtain the pure titania [51].

2.3 Photocatalytic reactions

The photocatalytic activity was evaluated following the degradation with respect to the time of two aqueous solutions of diuron (249 nm) and another of methyl parathion (275 nm), respectively. The conversion was measured by UV-Vis spectroscopy of the peaks of maximum absorbance for each pollutant. For this process was used a borosilicate Ace photocatalytic reactor that was enabled with a quartz recirculation system to maintain a constant reaction temperature of 20°C. The reaction total volume was 300 mL, employing 0.5 g/L as a catalyst concentration, constant stir and flow of 60 ml/seg atmospheric O₂. The total reaction time was 300 min. The reactions were carried out under sunlight, and the fully equipped reactor was placed on the roof of the laboratory building in full sunlight from 10:00 a.m. to 3:00 p.m.

3. Results and discussion

3.1 Results of characterization of TiO_2 doped with Ce^{3+} , Pr^{3+} , La^{3+} , Nd^{3+} , Sm^{3+} , Eu^{3+} , and Gd^{3+}

The diffuse reflectance spectra in the materials describe a change in the absorption band toward wavelengths corresponding to the visible region in all materials calcined at 500 (**Figure 1a** and **b**) and 800°C (**Figure 1c**). Due to the elimination of impurities, organic material and hydroxylated groups from the precursors in the synthesis, which use NH_4OH as hydrolysis catalyst and NO_3^- ions as precursors of the dopants, so it is expected that N atoms have been incorporated and eliminated by the effect of thermal treatment, causing a shift of the absorption bands toward longer [52], at the same time, this caused the production of oxygen vacancies, which also produced the same effect [53]. The spectra of **Figure 1a** present a greater absorption toward the visible for the solids doped with Pr 0.3%, Nd 0.1%, and 0.3%, however, for **Figure 1b**, the sample with Sm 0.3% is the one that greater absorption shows and in **Figure 1c**, the materials doped with Sm 0.3% and Gd 0.3% have this same behavior. In **Figure 1c**, it is evident that materials calcined at 800°C have a better absorption toward the visible, compared with those calcined at 500°C, due to the presence of the rutile crystalline phase, due to the increase in temperature in the thermal treatment, which consequently produces a decrease in the value of the band gap energy, the same happens with the sample of pure TiO_2 treated at 800°C. All doped materials already treated at 500 and 800°C show greater absorption than pure TiO_2 . The values of the E_g are shown in **Table 1**, here, it is observed that most of the samples treated at 500°C have a value ranging between 3.02 and 3.16 eV, including doped materials and pure TiO_2 , however, only the sample doped with Pr 0.3% decreased this value considerably (2.88 eV). With respect to the solids treated at 800°C, the photocatalyst doped with Eu 0.3% obtained the lowest value of E_g compared with all materials (2.5 eV).

Figure 2 shows the diffractograms corresponding to pure TiO_2 and TiO_2 -doped with rare earth ions, all thermally treated at 500°C. Only the anatase crystalline phase was detected in these samples presenting a low crystallinity (slightly amorphous), which is observed in the morphology by SEM in **Figure 6a**.

The results in Table 1 show that an average crystal size is 8.14 nm for the TiO_2 calcined at 500°C when introducing the dopants at the same treatment temperature the value decreases until 7.00 nm for the case of the catalyst with Sm 0.5%. In most of the samples doped to increase their content in the titania, the average crystal size decreases; this is due to the separation of the dopant in the limits of the crystal, which prevents its growth by not being able to be in contact with other crystals to grow by coalescence [54], except for the Nd and Pr, where their values are fixed

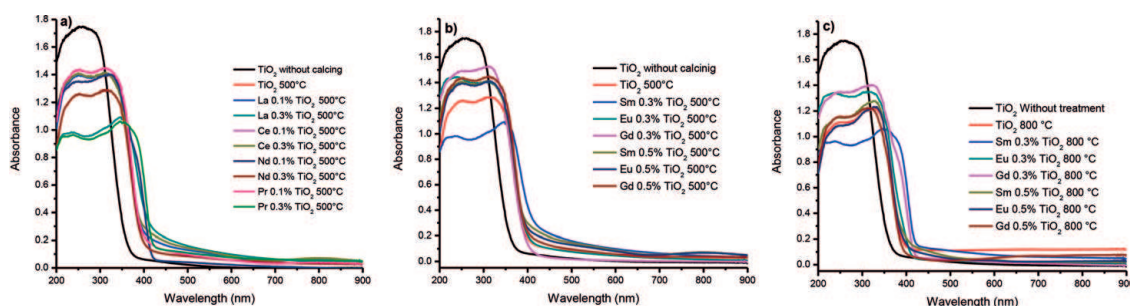


Figure 1. UV-Vis diffuse reflectance spectra of TiO_2 without treatment and TiO_2 (a) doped to 0.1 and 0.3% with La, Ce, Nd, and Pr calcinated at 500°C; (b) doped to 0.3 and 0.5% with Sm, Eu, and Gd calcinated at 500°C; (c) doped to 0.3 and 0.5% with Sm, Eu, and Gd calcinated at 800°C.

Samples	Specific Area Bet (m ² /g)	Pore Diameter (nm)	Average Crystal Size (nm)	% Mixture Phase Crystalline	Band Gap Energy (ev)
TiO ₂ 500 °C	78.71	7.91	9.91	100% A	3.02
TiO ₂ La0.1 500°C	90.10	9.50	8.41	100% A	3.07
TiO ₂ La0.3 500°C	119.00	9.50	7.21	100% A	3.10
TiO ₂ Ce0.1 500°C	98.01	9.50	8.41	100% A	3.00
TiO ₂ Ce0.3 500°C	109.04	9.50	9.01	100% A	3.10
TiO ₂ Nd0.1 500°C	99.00	7.81	8.41	100% A	2.98
TiO ₂ Nd0.3 500°C	111.06	7.70	8.41	100% A	3.00
TiO ₂ Pr0.1 500°C	99.09	7.80	8.41	100% A	3.05
TiO ₂ Pr0.3 500°C	112.01	7.70	8.41	100% A	2.88
TiO ₂ Sm0.1 500°C	105.70	7.70	8.25	100% A	3.16
TiO ₂ Sm0.3 500°C	109.50	9.40	7.07	100% A	3.10
TiO ₂ Sm0.5 500°C	95.91	8.42	7.00	100% A	3.09
TiO ₂ Eu0.1 500°C	101.80	9.42	9.91	100% A	3.09
TiO ₂ Eu0.3 500°C	100.50	9.49	8.25	100% A	3.09
TiO ₂ Eu0.5 500°C	104.70	7.87	8.20	100% A	3.08
TiO ₂ Gd0.1 500°C	113.32	7.6	8.25	100% A	3.23
TiO ₂ Gd0.3 500°C	93.91	9.43	8.25	100% A	3.11
TiO ₂ Gd0.5 500°C	92.48	8.14	8.21	100% A	3.07
TiO ₂ 800 °C	16.70	32.05	133.66	100% R	2.90
TiO ₂ Sm0.3 800°C	24.73	30.71	32.10 A 140.81 R	46.40% A 53.60% R	2.80
TiO ₂ Eu0.3 800°C	8.48	35.23	34.43 A 132.67 R	38.65% A 61.35% R	2.50
TiO ₂ Gd0.3 800°C	26.64	30.21	31.18 A 126.67 R	40.22% A 59.78% R	2.88

Table 1.
Results of characterization techniques applied to TiO₂ and doped TiO₂: N₂ physisorption, XRD and UV-Vis spectroscopy with RD.

and possibly with these ions to increase their content will no longer reduce their average crystal size. As mentioned above, the presence of rare earth ions inhibits the complete transformation of phases due to temperature; for our case, it happens at 800°C where catalysts stabilized at this temperature are present and clearly show mixtures of crystalline phases (anatase-rutile), and this is observed in **Figure 3**. A commercial sample of titania (P25-TiO₂) was compared with the materials calcined at the highest temperature with this technique. It was observed that the materials doped with rare earth ions showed a greater intensity in the peaks corresponding to the rutile phase, which describes a greater abundance of this phase and is less than 70% because this is the approximate percentage of rutile phase reported for this solid [55]. This can be corroborated with the results of **Table 1**, where the percentage of crystalline phase is described; here, the samples doped and calcined at 800°C indicate mixtures of phases with close proportions for Eu and Gd (40% A-60% R); however, for the Sm, the proportion percentage was almost equal (47% A-53% R). The above can also be confirmed according to the Raman spectra shown in

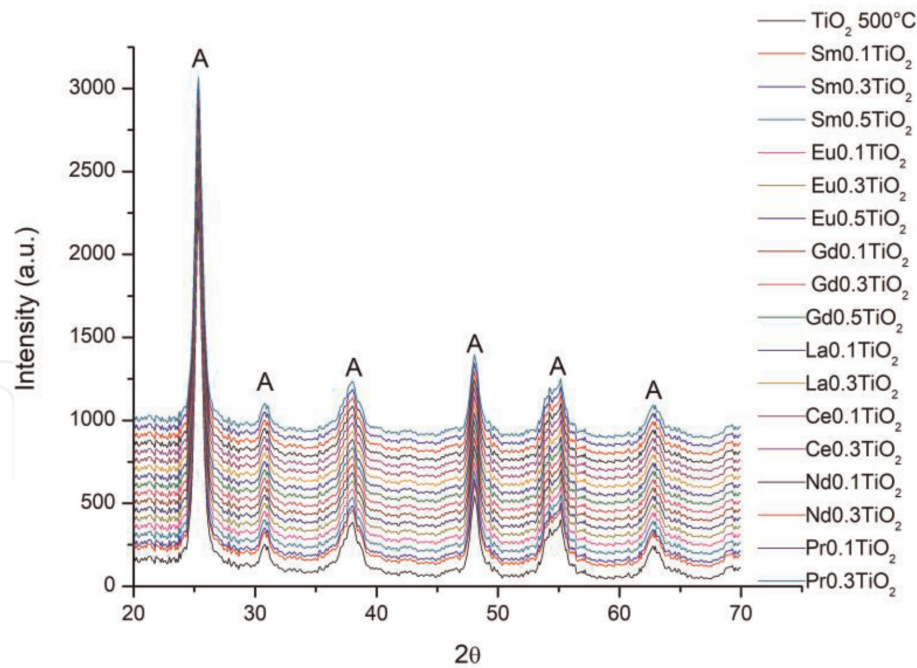


Figure 2.
XRD patterns of pure TiO₂ and doped TiO₂ with rare earth thermally treated to 500°C.

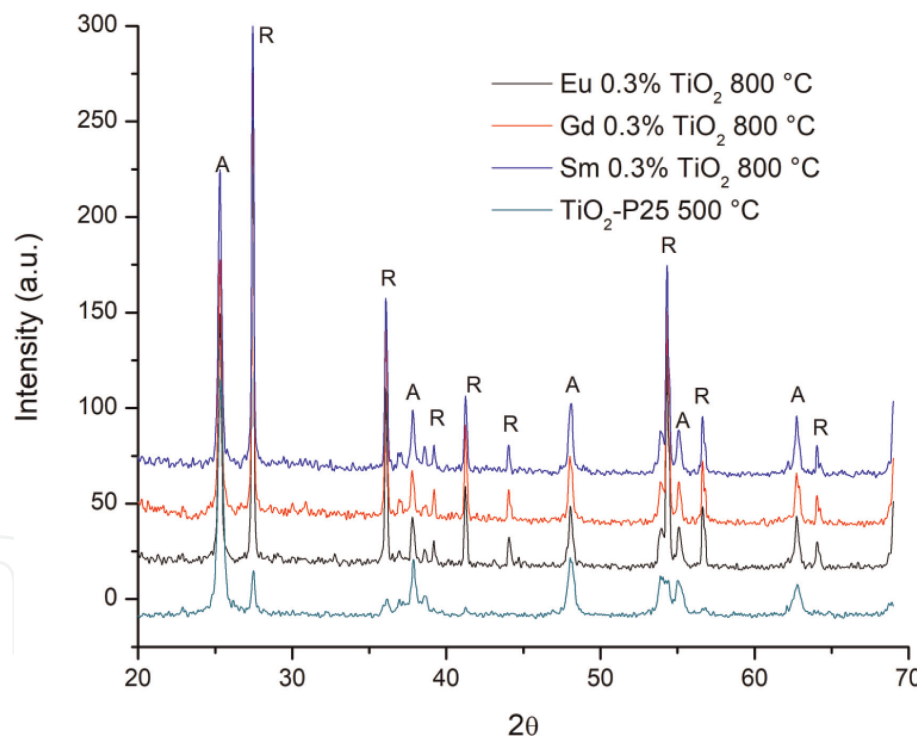


Figure 3.
XRD patterns of P25-TiO₂ and doped TiO₂ with rare earth thermally treated to 800°C.

Figure 4, in which the peaks corresponding to the anatase and rutile phases respectively are described. The phase mixtures at high temperatures can be explained due to the connection between the Ti⁴⁺ (octahedral) and RE³⁺ (tetrahedral) ions, where the Ti⁴⁺ ions replace the surface RE³⁺ ions in the network the rare earth oxide to form sites tetragonal of Ti, the interaction between atoms of Ti⁴⁺ octahedral and Ti⁴⁺ tetrahedral prevents the transformation of phases in the thermal treatment [56]. The average crystal size for these samples is also found in **Table 1** and calculated individually for each crystalline phase. With respect to the anatase phase, the highest value was presented by the sample doped with Eu (34.43 nm), which is

more than three times greater than the sample of pure titania at 500°C. However, the material doped with Sm obtained the highest average crystal size for the rutile phase (140.81 nm).

Figure 5 shows the adsorption-desorption isotherms of the materials calcined at 500°C. It is noteworthy that the incorporation of the dopant into TiO₂ generates greater physical adsorption by increasing the relative pressure, explained by a possible uniform surface dispersion of the dopant, which demonstrates the increase in the specific area with respect to pure TiO₂ and the capacity of the dopant. Rare

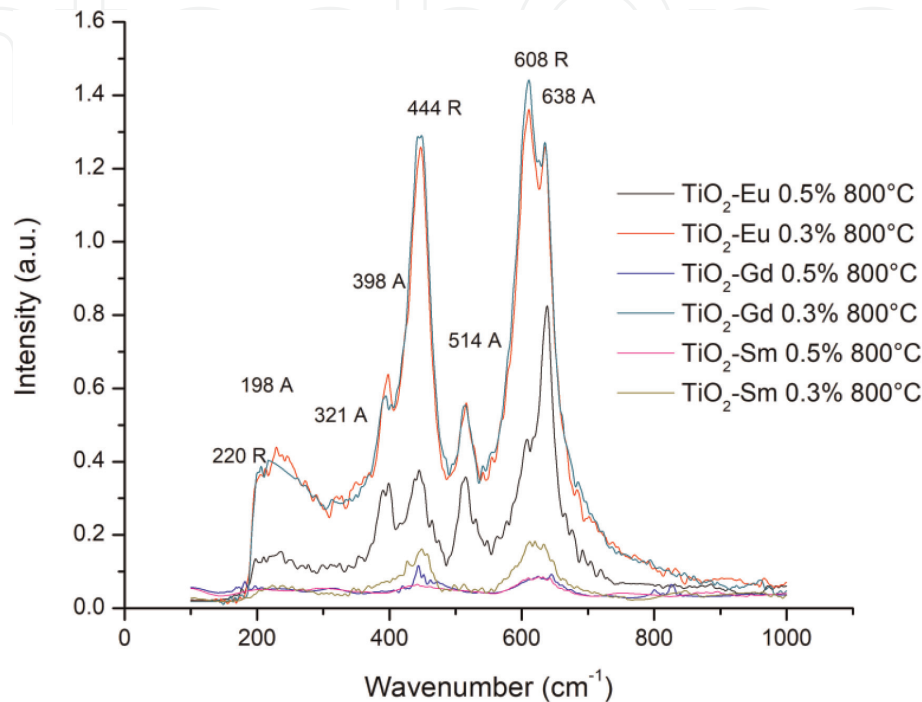


Figure 4.
Raman spectra of TiO₂ doped with Sm, Eu, and Gd, calcinated at 800°C.

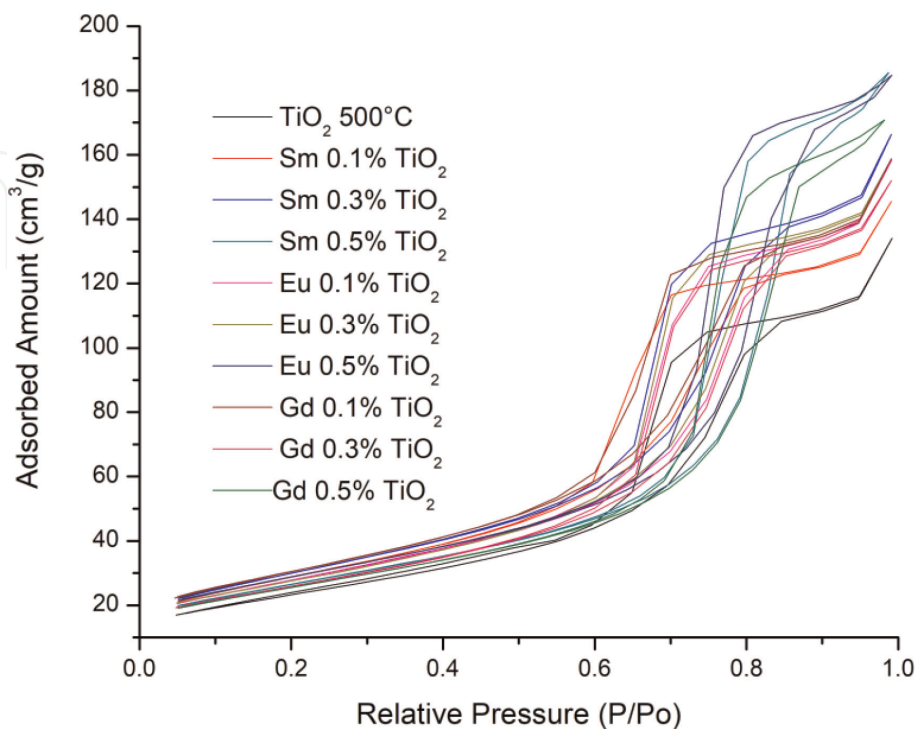


Figure 5.
Adsorption-desorption isotherms of TiO₂ and doped TiO₂ with Sm, Eu, and Gd calcinated at 500°C.

earth ions to form complexes with several Lewis bases. It is observed that all the isotherms have a type IV behavior according to the IUPAC classification, which is a characteristic of mesoporous solids and has multiple layer adsorption mechanism, with a hysteresis loop of type A according to the same organism, which indicates the description of mesoporous solids with capillaries in tubular form and ink cans; these samples have a desorption of similar geometric shape although their adsorption varied with respect to the metal and the amount of dopant.

The specific area values of the pure, doped, and calcined catalysts at 500 and 800°C are compiled in **Table 1**. As expected, the presence of the dopants in the titania increases the specific area for all materials treated at 500°C, which previously had already been described with other materials [51]. The value of this parameter was between 90.10 and 119.50 m²/g, the sample doped with Ce 0.3% presented the highest value, and this increase can be attributed to (1) the high dispersion that had the rare earth ions and this can be seen in **Figure 6b** with the image describing the elemental dispersion of Sm at 0.3% in titania, which also manifests with all doping ions, (2) to the impediment of rare earth ions to enter the lattice titania due to the large size of its ions, (3) the low amount of dopant that was used and (4) the reduction in the size of the crystal. This confirms that the rare earth ions inhibit the sintering of TiO₂ [57].

The thermal transformation to rutile in the titania decreases considerably the specific area to 800°C and therefore, increases its crystallinity and the sintering process, but when inserting Sm and Eu to 0.3%, the area increases due to the formation of mixtures of crystalline phases, distorting the surface of the titania due to the presence of dopants. The titania catalyst doped with Eu at 0.3% and calcined at 800°C does not increase its specific area; it is the only one that shows a value below pure TiO₂; this possibly at the low percentage ratio that it has anatase phase.

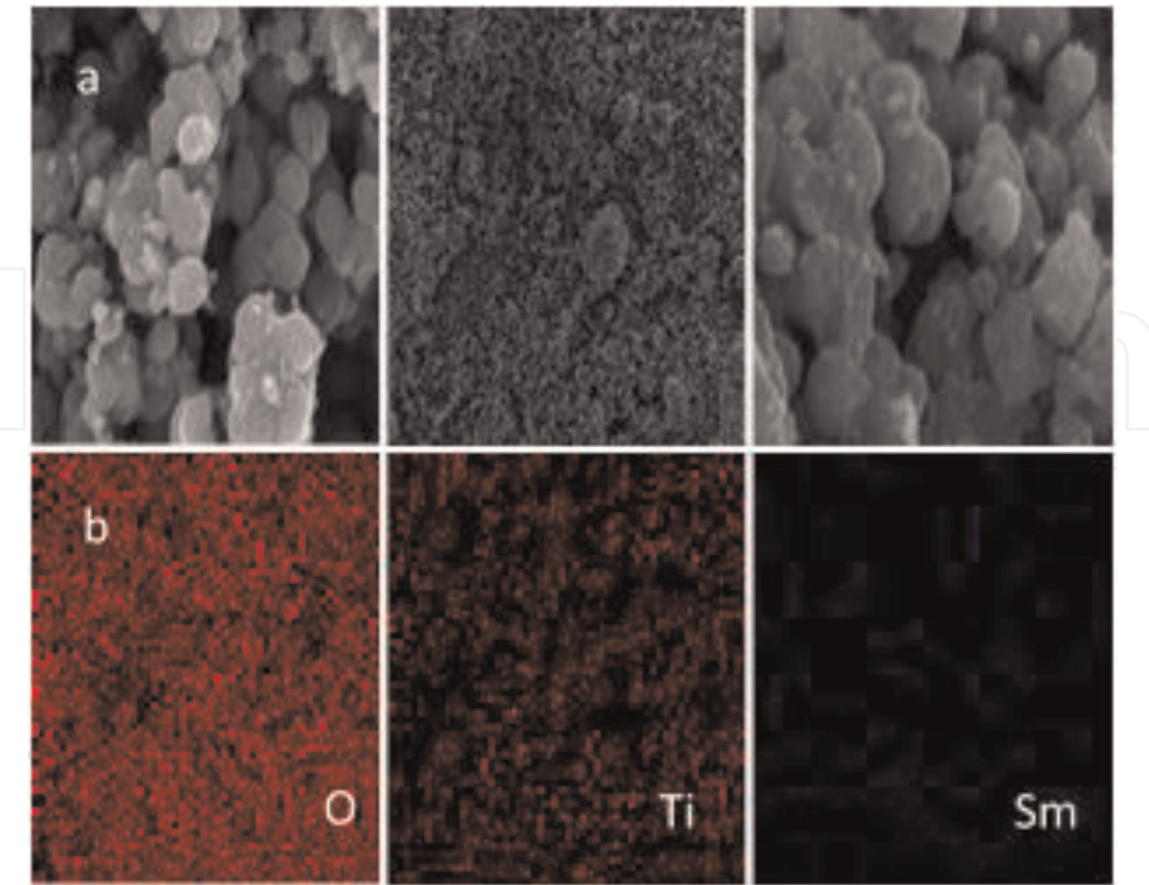


Figure 6.
Images obtained by SEM to the Sm 0.3 TiO₂ 500°C: (a) morphology and (b) elemental mapping.

The pore diameter showed an increase with respect to pure TiO₂ with samples doped with La, Ce at different contents, with Eu at 0.1 and 0.3%, with Sm 0.3 and 0.5%, and with Gd 0.3 and 0.5% all calcined at 500°C. This increase is attributed to the fusion of small pores present in the anatase phase to form large pores or stacked cavities. However, the reduction in the value of this parameter is explained by the possible blocking of porous cavities by the dopants. Similarly, at 800°C, the materials showed similar behavior, but to these conditions, the increase in the pore diameter is due to pore coalescence during calcination [51].

3.2 Results of photocatalytic tests of diuron using TiO₂-RE

The photocatalytic activity under sunlight in the photodegradation of diuron is described in **Figure 7**. All materials doped and calcined at 500°C obtained a higher yield than photolysis, pure TiO₂ and P25-TiO₂ (**Figure 7a**). This behavior is directly related to the high dispersion of dopants, which superficially modifies the titania, considerably increasing its specific area. The materials doped with La and Ce 0.1%, respectively, are the most active of the series when starting the dopant content, show an increase in the volume of pores, which indicates that the dispersion of these dopants do not obstruct the porous cavities, generating a porous material that has greater contact with the polluting solution, the opposite occurs with the rest of

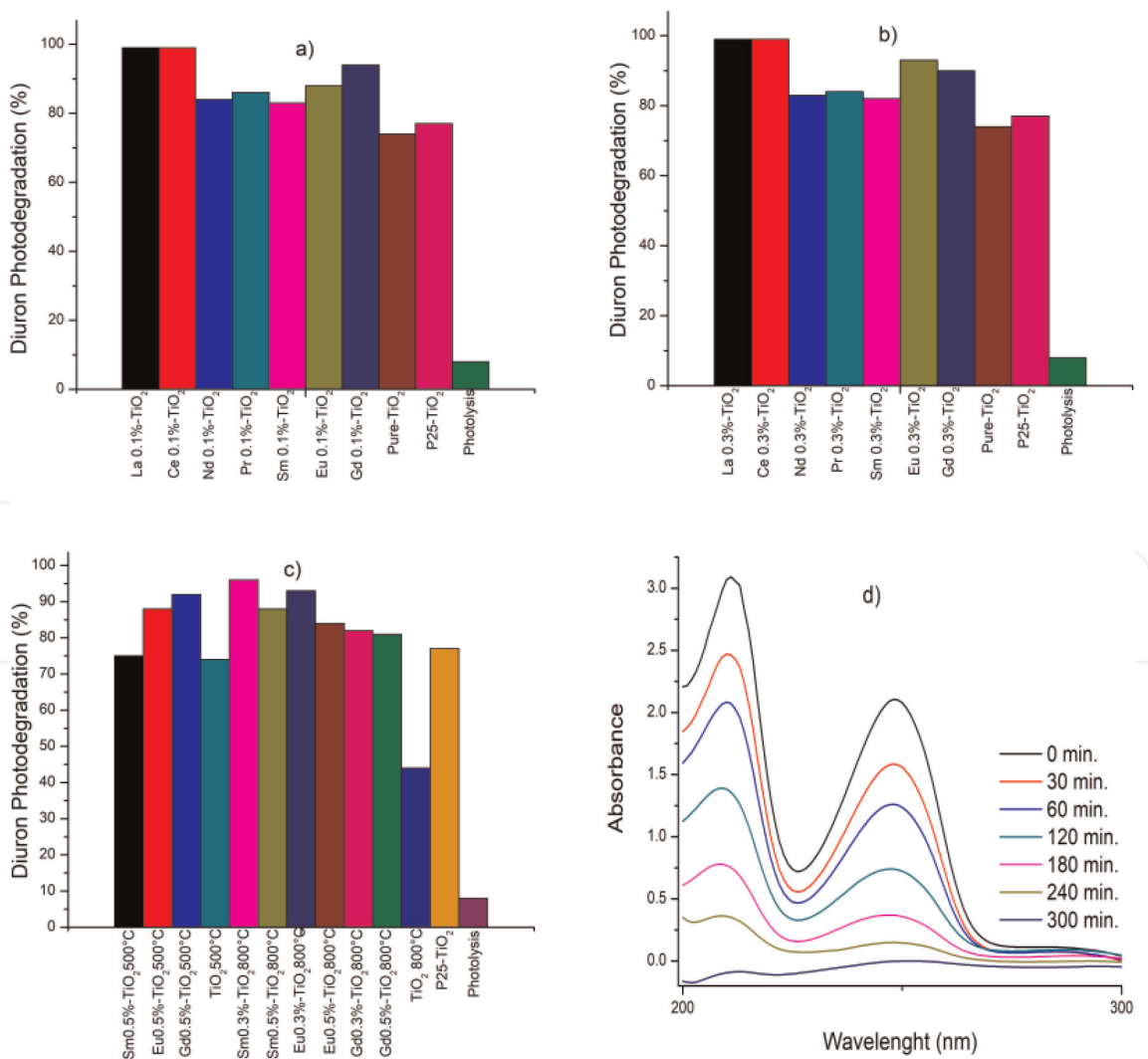


Figure 7. Photocatalytic degradation of diuron using solar light: (a) doped photocatalyst to 0.1% at 500°C. (b) Doped photocatalyst to 0.3% at 500°C. (c) Doped photocatalyst to 0.5% at 500°C and doped photocatalyst to 0.3–0.5% at 800°C. (d) Solar photodegradation of diuron with Ce 0.1% TiO₂ 500°C.

the doping ions, which upon insertion decrease the pore volume and its photoactivity decreases. For the sample with Eu, although it also increases its pore volume with respect to pure titania, its activity declines considerably and has the worst photocatalytic performance, when contrasting this phenomenon with the average particle sizes. It was found that this material maintains the same particle size; therefore, it can be attributed that photocatalytic activity in this material depends on the average particle size.

When increasing the content to 0.3% of the dopants in the titania, the materials doped with Eu and Gd do not increase the specific area with respect to the photocatalysts, in which the samples doped only with La, Ce, and Sm increase their photocatalytic performance, as seen in **Figure 7b**. The first two conserve the same pore diameter, showing a good dispersion by augmenting the dopant content that consequently raises the specific area, without blocking pores as reported in other investigations [19]. In the sample with Sm at this content, the dispersion improves remarkably with respect to 0.1%, which was observed in **Figure 6b** in the elemental mapping by EDS, which increases the pore diameter in the material. The tendency in the size of crystal when increasing concentration of dopant describes a reduction and conservation in values of this parameter, which already has been previously reported [54]; only the material doped with Ce increases this value, but not in a way significant and still showing a smaller size with respect to pure titania.

In **Figure 7c**, it is observed that the increase dopant content to 0.5% decrease photocatalytic efficiency; this gives us an idea of what is the content and the ideal ions of rare earth as dopants in the titania for solar photodegradation in aqueous medium of the diuron (**Figure 7d**), as in other investigations, at higher dopant concentrations, the pore diameter and average crystal size decrease [58]. Nevertheless, if the content of doping ions is excessively high, the recombination process of the photo-generated becomes easier, which led to the lower photocatalytic activity of titania. The photoactivity of some samples calcined at 800°C, presented a better efficiency than pure TiO₂ and P25-TiO₂; the trend of the specific area describes an increase with the presence of dopants, but with Eu, this parameter decreased considerably to a value below pure titania. The photocatalyst with Sm 0.3% was the most active, followed by Eu and Gd at this treatment temperature; this is attributed mainly to the presence of mixtures of crystalline phases (anatase-rutile), which incorporates Sm; the ratio of this mixture indicates a higher content of anatase (about 46%), as described above. This phase is more active than rutile and has a higher anatase ratio than that reported for P25-TiO₂ (30% approx.); therefore, the performance is better. However, this same sample has a crystal size for the greater rutile phase compared to the rest of the materials, which indicates that the growth of the rutile crystals is directly proportional to the photocatalytic activity of the materials.

The materials doped and thermally stabilized at 500°C more active in the previous reaction, were selected to evaluate them photocatalytically under sunlight in the degradation of an organophosphorus insecticide (methyl parathion), to analyze the effect that photocatalysts have on different aqueous pollutants with different functional groups (phenylurea and thiophosphate). Although materials doped at 0.1 and 0.3% with La and Ce obtained similar yields, those with the least amount of dopant were chosen.

3.3 Results of photocatalytic tests of methyl parathion using TiO₂-RE

The photocatalytic behavior of the catalysts chosen for this test is described in **Figure 8a**; in **Figure 8b**, the photodegradation of methyl parathion with respect to time is shown in the most photoactive material of this series of materials doped and

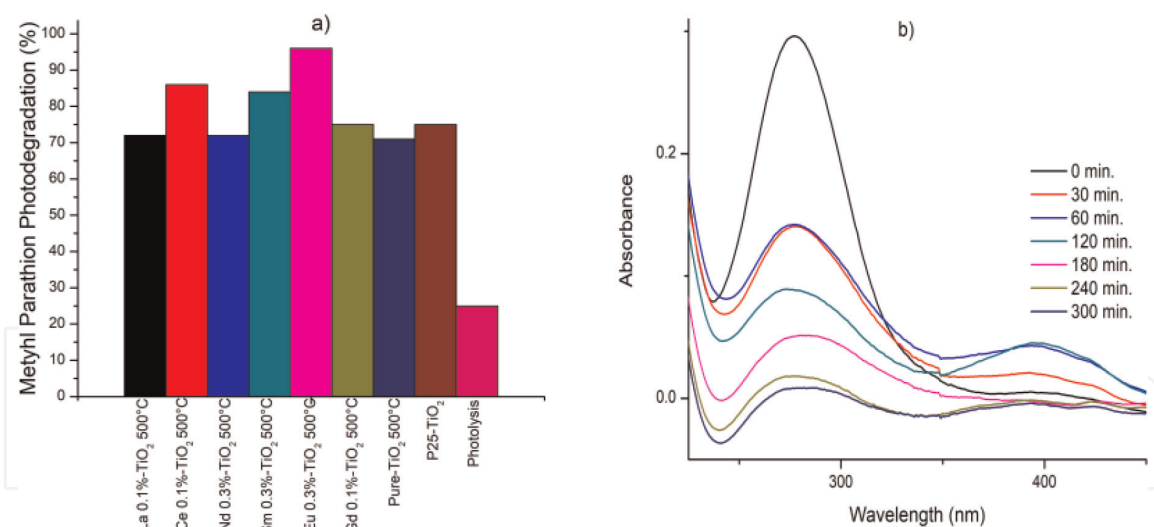


Figure 8. Photocatalytic degradation of methyl parathion using solar light: (a) La 0.1% TiO₂, Ce 0.1% TiO₂, Nd 0.3% TiO₂, Sm 0.3% TiO₂, Eu 0.3% TiO₂, Gd 0.1% TiO₂, pure TiO₂, P25-TiO₂ and photolysis. (b) Solar photodegradation of methyl parathion with Eu 0.3% TiO₂ 500°C.

calcined at 500°C. A different trend is observed when comparing the activity of the materials with the previous model molecule (diuron). The conversion by photolysis without catalyst was around 25%; however, conversions are reached above 95% with TiO₂ doped with Eu at 0.3% and with the other catalysts, the conversions exceed 70%. Only samples doped with Eu 0.3%, Ce 0.1%, and Sm 0.3% were more active than P25-titania. The value of the average diameter of pores in these materials increased and was compared with the pure titania; this increment also happened with the doped catalyst with La, but as its specific area was the lowest, this reduced its photoactivity. This seems to indicate that the presence of pores and specific area large, allows a better diffusion between the polluting solution and the photocatalyst to increase the photoactivity of TiO₂ doped with rare earth ions. With respect to the average crystal size, all materials decrease this value due to the presence of rare earth ions, which inhibit the growth of crystals in the process of synthesis and thermal stabilization. Finally, it can be stated that there is an affinity between the doped ions in the titania and the main functional groups of the molecules used for the photodegradation under sunlight. With phenylurea (diuron), solar photodegradation was more pronounced with the materials doped with La and Ce, meanwhile, for the thiophosphate (methyl parathion), the process of solar photo-oxidation had a greater affinity for the Eu.

4. Conclusions

The rare earth doping ions improve the textural, structural, electronic, and photocatalytic properties in TiO₂. Due to the method of preparation and the treatment temperature, possibly the presence of N and the elimination of impurities produced a change in the absorption bands, which allows the titania to have a better photocatalytic behavior under sunlight. At 500°C, the materials present 100% of the anatase crystalline structure, the ideal amount of dopant was 0.1% and the most active rare earth ions were La and Ce in the diuron solar photodegradation. The increase in temperature of thermal treatment (800°C) showed the presence of mixtures of crystalline phases, which have a greater abundance of anatase, compared to P25-TiO₂, where the catalyst doped with Sm 0.3% obtained the best performance. Photocatalysts treated at 500°C with greater activity in diuron

degradation were chosen to evaluate their solar photoactivity with a second pesticide (methyl parathion). Under these conditions, an affinity was found for the dopant ions in titania and the functional groups of the contaminating molecules (phenylurea and thiophosphate). Solar photodegradation of diuron was more effective with La and Ce, while for methyl parathion it was Eu at 0.3%.

Acknowledgements

The authors thank the National Council for Science and Technology (CONACYT) for financing the project 132648 and thank the Universidad Juárez Autónoma de Tabasco for PFCE-DACB Project and PRODEP Program.

Conflict of interest


The authors declare no conflicts of interest.

Author details

Juan C. Arévalo Pérez*, José Gilberto Torres Torres, Durvel de la Cruz Romero, Hermicenda Perez-Vidal, Maria Antonia Lunagomez Rocha, Ignacio Cuauhtémoc López, Adrian Cervantes Uribe and Zenaida Guerra Que Laboratory of Catalytic Nanomaterials Applied to the Development of Energy Sources and Environmental Remediation, Applied Science and Technology Research Center of Tabasco (CICTAT), Juarez Autonomous University of Tabasco, DACB, Cunduacan, Tabasco, México

*Address all correspondence to: juan.carlos.arevalo.jcap@gmail.com

IntechOpen

© 2019 The Author(s). Licensee IntechOpen. This chapter is distributed under the terms of the Creative Commons Attribution License (<http://creativecommons.org/licenses/by/3.0>), which permits unrestricted use, distribution, and reproduction in any medium, provided the original work is properly cited. 

References

- [1] Cerejeira MJ, Viana P, Batista S, Pereira T, Silva E, Val MJ, et al. Pesticides in Portuguese surface and ground waters. *Water Research*. 2003; **37**:1055-1063. DOI: 10.1016/S0043-1354(01)00462-6
- [2] Parimi S, Meinke LJ, Wade French B, Chandler LD, Siegfried BD. Stability and persistence of aldrin and methyl-parathion resistance in western corn rootworm populations (Coleoptera: Chrysomelidae). *Crop Protection*. 2006; **25**:269-274. DOI: 10.1016/j.cropro.2005.04.017
- [3] Zhang J, Zheng Z, Zhao T, Zhao Y, Wang L, Zhong Y, et al. Radiation-induced reduction of diuron by gamma-ray irradiation. *Journal of Hazardous Materials*. 2008; **151**:465-472
- [4] Taylor P, Krishna KR, Philip L. Biodegradation of lindane, methyl parathion and carbofuran by various enriched bacterial isolates. *Journal of Environmental Science and Health, Part B*. 2008; **37**:41. DOI: 10.1080/03601230701795155
- [5] Kim TS, Kim JK, Choi K, Stenstrom MK, Zoh KD. Degradation mechanism and the toxicity assessment in TiO₂ photocatalysis and photolysis of parathion. *Chemosphere*. 2006; **62**:926-933. DOI: 10.1016/j.jss.2005.06.046
- [6] Saqib N, Adnan R, Shah I. A mini-review on rare earth metal-doped TiO₂ for photocatalytic remediation of wastewater. *Environmental Science and Pollution Research*. 2016; **15**:15941-15951. DOI: 10.1007/s11356-016-6984-7
- [7] Carraway ER, Hoffman AJ, Hoffmann MR. Photocatalytic oxidation of organic-acids on quantum-sized semiconductor colloids. *Environmental Science & Technology*. 1994; **28**:786-793. DOI: 10.1021/es00054a007
- [8] Choi H, Antoniou MG, Pelaez M, De La Cruz AA, Shoemaker JA, Dionysiou DD. Mesoporous nitrogen-doped TiO₂ for the photocatalytic destruction of the cyanobacterial toxin microcystin-LR under visible light irradiation. *Environmental Science and Technology*. 2007; **41**:7530-7535. DOI: 10.1021/es0709122
- [9] Wilke K, Breuer HD. The influence of transition metal doping on the physical and photocatalytic properties of titania. *Journal of Photochemistry and Photobiology A: Chemistry*. 1999; **121**:49-53. DOI: 10.1016/S1010-6030(98)00452-3
- [10] Pan X, Xu YJ. Defect-mediated growth of noble-metal (Ag, Pt, and Pd) nanoparticles on TiO₂ with oxygen vacancies for photocatalytic redox reactions under visible light. *Journal of Physical Chemistry C*. 2013; **117**:17996-18005. DOI: 10.1021/jp4064802
- [11] Ma Y, Zhang J, Tian B, Chen F, Wang L. Synthesis and characterization of thermally stable Sm, N co-doped TiO₂ with highly visible light activity. *Journal of Hazardous Materials*. 2010; **182**:386-393. DOI: 10.1016/j.jhazmat.2010.06.045
- [12] Chen FY, Cao WK, He SY, Wang BH, Zhang YM. Synthesis, characterization and thermochemistry properties of RE(III) and 2-oxo-propionic acid salicyloyl hydrazone complexes. *Acta Physico-Chimica Sinica*. 2006; **22**:280-285. DOI: 10.1016/S1872-1508(06)60003-X
- [13] Mazierski P, Mikolajczyk A, Bajorowicz B, Malankowska A, Zaleska-Medynska A, Nadolna J. The role of lanthanides in TiO₂ based photocatalysis: A review. *Applied Catalysis B: Environmental*. 2018; **233**:301-317. DOI: 10.1016/j.apcatb.2018.04.019

- [14] Zhang W, Yang S, Li J, Gao W, Deng Y, Dong W, et al. Applied catalysis B: Environmental visible to ultraviolet Upconversion: Energy transfer, material matrix, and synthesis strategies. *Applied Catalysis B, Environmental*. 2017;**206**: 89-103. DOI: 10.1016/j.apcatb.2017.01.023
- [15] Lin J, Yu JC. An investigation on photocatalytic activities of mixed TiO₂ rare earth oxides for the oxidation of acetone in air. *Journal of Photochemistry and Photobiology A: Chemistry*. 1998;**116**:63-67. DOI: 10.1016/S1010-6030(98)00289-5
- [16] Yu Y, Chen G, Zhou Y, Han Z. Recent advances in rare-earth elements modification of inorganic semiconductor-based photocatalysts for efficient solar energy conversion: A review. *Journal of Rare Earths*. 2015;**33**: 453-462. DOI: 10.1016/S1002-0721(14)60440-3
- [17] Zhu J, Xie J, Chen M, Jiang D, Wu D. Low temperature synthesis of anatase rare earth doped titania-silica photocatalyst and its photocatalytic activity under solar-light. *Colloids and Surfaces A: Physicochemical and Engineering Aspects*. 2010;**355**:178-182. DOI: 10.1016/j.colsurfa.2009.12.016
- [18] Lin L, Chai Y, Yang Y, Wang X, He D, Tang Q, et al. Hierarchical Gd-La codoped TiO₂ microspheres as robust photocatalysts. *International Journal of Hydrogen Energy*. 2013;**38**:2634-2640. DOI: 10.1016/j.ijhydene.2012.11.100
- [19] El-Bahy ZM, Ismail AA, Mohamed RM. Enhancement of titania by doping rare earth for photodegradation of organic dye (direct blue). *Journal of Hazardous Materials*. 2009;**166**:138-143. DOI: 10.1016/j.jhazmat.2008.11.022
- [20] Baiju KV, Periyat P, Shajesh P, Wunderlich W, Manjumol KA, Smitha VS, et al. Mesoporous gadolinium doped titania photocatalyst through an aqueous sol-gel method. *Journal of Alloys and Compounds*. 2010;**505**: 194-200. DOI: 10.1016/j.jallcom.2010.06.028
- [21] Yan QZ, Su XT, Huang ZY, Ge CC. Sol-gel auto-igniting synthesis and structural property of cerium-doped titanium dioxide nanosized powders. *Journal of the European Ceramic Society*. 2006;**26**:915-921. DOI: 10.1016/j.jeurceramsoc.2004.11.017
- [22] Liang CH, Li FB, Liu CS, Lü JL, Wang XG. The enhancement of adsorption and photocatalytic activity of rare earth ions doped TiO₂ for the degradation of Orange I. *Dyes and Pigments*. 2008;**76**:477-484. DOI: 10.1016/j.dyepig.2006.10.006
- [23] Castillo MA, Felis N, Aragón P, Cuesta G, Sabater C. Biodegradation of the herbicide diuron by streptomycetes isolated from soil. *International Biodeterioration and Biodegradation*. 2006;**58**:196-202. DOI: 10.1016/j.ibiod.2006.06.020
- [24] Giacomazzi S, Cochet N. Environmental impact of diuron transformation: A review. *Chemosphere*. 2004;**56**:1021-1032. DOI: 10.1016/j.chemosphere.2004.04.061
- [25] Macounová K, Krýsová H, Ludvík J, Jirkovský J. Kinetics of photocatalytic degradation of diuron in aqueous colloidal solutions of Q-TiO₂. *Journal of Photochemistry and Photobiology A: Chemistry*. 2003;**156**:273-282. DOI: 10.1016/S1010-6030(02)00091-6
- [26] Katsumata H, Sada M, Nakaoka Y, Kaneco S, Suzuki T, Ohta K. Photocatalytic degradation of diuron in aqueous solution by platinized TiO₂. *Journal of Hazardous Materials*. 2009;**171**:1081-1087. DOI: 10.1016/j.jhazmat.2009.06.110
- [27] Pino N, Peñuela G. Simultaneous degradation of the pesticides methyl

parathion and chlorpyrifos by an isolated bacterial consortium from a contaminated site. *International Biodeterioration and Biodegradation*. 2011;**65**:827-831. DOI: 10.1016/j.ibiod.2011.06.001

[28] Ragnarsdottir K. Environmental fate and toxicology of organophosphate pesticides. *Journal of the Geological Society*. 2000;**157**:859-876. DOI: 10.1007/978-3-319-03777-6_3

[29] Evgenidou E, Konstantinou I, Fytianos K, Poullos I, Albanis T. Photocatalytic oxidation of methyl parathion over TiO₂ and ZnO suspensions. *Catalysis Today*. 2007;**124**: 156-162. DOI: 10.1016/j.cattod.2007.03.033

[30] Senthilnathan J, Philip L. Photodegradation of methyl parathion and dichlorvos from drinking water with N-doped TiO₂ under solar radiation. *Chemical Engineering Journal*. 2011;**172**:678-688. DOI: 10.1016/j.cej.2011.06.035

[31] Zhang T, Oyama T, Horikoshi S, Zhao J, Hidaka H, Serpone N. Significant effect of lanthanide doping on the texture and properties of nanocrystalline mesoporous TiO₂. *Journal of Solid State Chemistry*. 2004;**177**:3490-3498. DOI: 10.1016/j.jssc.2004.05.026

[32] Bossmann SH, Braun AM. Lanthanide oxide-doped titanium dioxide photocatalysts: Novel photocatalysts for the enhanced degradation of p-chlorophenoxyacetic acid. *Environmental Science Technology*. 2001;**35**:1544-1549. DOI: 10.1021/es001613e

[33] Yurtsever HA, Çiftçioğlu M. The effect of rare earth element doping on the microstructural evolution of sol-gel titania powders. *Journal of Alloys and Compounds*. 2016;**695**:1336-1353. DOI: 10.1016/j.jallcom.2016.10.275

[34] Di S, Guo Y, Lv H, Yu J, Li Z. Microstructure and properties of rare earth CeO₂-doped TiO₂ nanostructured composite coatings through micro-arc oxidation. *Ceramics International*. 2015;**41**:6178-6186. DOI: 10.1016/j.ceramint.2014.12.134

[35] Wojcieszak D. Analysis of Eu-effect on stabilization of the TiO₂-anatase structure in high temperature and photoluminescence efficiency for the coatings as-deposited in magnetron sputtering process. *Applied Surface Science*. 2017;**421**:128-133. DOI: 10.1016/j.apsusc.2017.01.040

[36] Labreche F, Berbadj A, Brihi N, Karima R, Jamoussi B. Green photoluminescence, structural and optical properties of Nd-TiO₂ thin films. *Optik*. 2018;**172**:63-71. DOI: 10.1016/j.ijleo.2018.06.131

[37] Borlaf M, Colomer MT, Moreno R, Ortiz AL. Rare earth-doped TiO₂ nanocrystalline thin films: Preparation and thermal stability. *Journal of the European Ceramic Society*. 2014;**34**: 4457-4462. DOI: 10.1016/j.jeurceramsoc.2014.07.008

[38] Hassan MS, Amna T, Yang O, Kim H, Khil M. TiO₂ nanofibers doped with rare earth elements and their photocatalytic activity. *Ceramics International*. 2012;**38**:5925-5930. DOI: 10.1016/j.ceramint.2012.04.043

[39] Mazierski P, Lisowski W, Grzyb T, Winiarski MJ, Klimczuk T, Mikołajczyk A, et al. Enhanced photocatalytic properties of lanthanide-TiO₂ nanotubes: An experimental and theoretical study. *Applied Catalysis B, Environmental*. 2016;**205**:376-385. DOI: 10.1016/j.apcatb.2016.12.044

[40] Jian Z, Pu Y, Fang J, Ye Z. Microemulsion synthesis of nanosized TiO₂ particles doping with rare-earth and their photocatalytic activity. *Photochemistry and Photobiology*.

2010;**86**:1016-1021. DOI: 10.1111/j.1751-1097.2010.00773.x

[41] Bandi VR, Raghavan CM, Grandhe BK, Kim SS, Jang K, Shin DS, et al. Synthesis, structural and optical properties of pure and rare-earth ion doped TiO₂ nanowire arrays by a facile hydrothermal technique. *Thin Solid Films*. 2013;**547**:207-211. DOI: 10.1016/j.tsf.2013.03.039

[42] Tobaldi DM, Pullar RC, Škapin AS, Seabra MP, Labrincha JA. Visible light activated photocatalytic behaviour of rare earth modified commercial TiO₂. *Materials Research Bulletin*. 2014;**50**: 183-190. DOI: 10.1016/j.materresbull.2013.10.033

[43] Zhang J, Wu W, Yan S, Chu G, Zhao S, Wang X, et al. Enhanced photocatalytic activity for the degradation of rhodamine B by TiO₂ modified with Gd₂O₃ calcined at high temperature. *Applied Surface Science*. 2015;**344**:249-256. DOI: 10.1016/j.apsusc.2015.03.078

[44] Akpan UG, Hameed BH. The advancements in sol-gel method of doped-TiO₂ photocatalysts. *Applied Catalysis A: General*. 2010;**375**:1-11. DOI: 10.1016/j.apcata.2009.12.023

[45] Dominguez RD, Alarcón-Flores G, Aguilar-Frutis M, Sánchez-Alarcón RI, Falcony C, Dorantes-Rosales HJ, et al. Effect on the stabilization of the anatase phase and luminescent properties of samarium-doped TiO₂ nanocrystals prepared by microwave irradiation. *Journal of Alloys and Compounds*. 2016;**687**:121-129. DOI: 10.1016/j.jallcom.2016.06.083

[46] Su W, Chen J, Wu L, Wang X, Wang X, Fu X. Visible light photocatalysis on praseodymium (III)-nitrate modified TiO₂ prepared by an ultrasound method. *Applied Catalysis B: Environmental*. 2008;**77**:264-271. DOI: 10.1016/j.apcatb.2007.04.015

[47] Zhang W, Zou L, Wang L. Photocatalytic TiO₂/adsorbent nanocomposites prepared via wet chemical impregnation for wastewater treatment: A review. *Applied Catalysis A: General*. 2009;**371**:1-9. DOI: 10.1016/j.apcata.2009.09.038

[48] Arévalo Pérez JC, Torres JG, Cervantes Uribe A, Pérez Vidal H, Cordero García A, Izquierdo Colorado A, et al. Use of multivariable analysis (ANOVA) to compare irradiation sources on diuron destruction by photocatalysis using TiO₂-P25 impregnated with Sm³⁺, Eu³⁺ and Gd³⁺. *Journal of Chemical Engineering & Process Technology*. 2018;**9**:1-8. DOI: 10.4172/2157-7048.1000374

[49] Spurr RA, Myers H. Quantitative analysis of anatase-rutile mixtures with an X-ray diffractometer. *Analytical Chemistry*. 1957;**29**:760-762. DOI: 10.1021/ac60125a006

[50] De la Cruz D, Arévalo JC, Torres G, Bautista Margulis RG, Ornelas C, Aguilar-elguézabal A. TiO₂ doped with Sm³⁺ by sol-gel : Synthesis, characterization and photocatalytic activity of diuron under solar light. *Catalysis Today*. 2011;**166**:152-158. DOI: 10.1016/j.cattod.2010.08.023

[51] De la Cruz Romero D, Torres GT, Arévalo JC, Gomez R, Aguilar-Elguézabal A. Synthesis and characterization of TiO₂ doping with rare earths by sol-gel method: Photocatalytic activity for phenol degradation. *Journal of Sol-Gel Science and Technology*. 2010;**56**:219-226. DOI: 10.1007/s10971-010-2297-3

[52] Silveyra R, De La Torre SL, Flores WA, Martínez VC, Elguézabal AA. Doping of TiO₂ with nitrogen to modify the interval of photocatalytic activation towards visible radiation. *Catalysis Today*. 2005;**107-108**:602-605. DOI: 10.1016/j.cattod.2005.07.023

[53] Yamada K, Yamane H, Matsushima S, Nakamura H, Ohira K, Kouya M, et al. Effect of thermal treatment on photocatalytic activity of N-doped TiO₂ particles under visible light. *Thin Solid Films*. 2008;**516**:7482-7487. DOI: 10.1016/j.tsf.2008.03.041

[54] Zhang Y, Xu H, Xu Y, Zhang H, Wang Y. The effect of lanthanide on the degradation of RB in nanocrystalline Ln/TiO₂ aqueous solution. *Journal of Photochemistry and Photobiology A: Chemistry*. 2005;**170**:279-285. DOI: 10.1016/j.jphotochem.2004.09.001

[55] Du P, Bueno-López A, Verbaas M, Almeida AR, Makkee M, Moulijn JA, et al. The effect of surface OH-population on the photocatalytic activity of rare earth-doped P25-TiO₂ in methylene blue degradation. *Journal of Catalysis*. 2008;**260**:75-80. DOI: 10.1016/j.jcat.2008.09.005

[56] Hwang DW, Lee JS, Li W, Oh SH. Electronic band structure and photocatalytic activity of Ln₂Ti₂O₇ (Ln = La, Pr, Nd). *Journal of Physical Chemistry B*. 2003;**107**:4963-4970. DOI: 10.1021/jp034229n

[57] Saif M, Abdel-Mottaleb MSA. Titanium dioxide nanomaterial doped with trivalent lanthanide ions of Tb, Eu and Sm: Preparation, characterization and potential applications. *Inorganica Chimica Acta*. 2007;**360**:2863-2874. DOI: 10.1016/j.ica.2006.12.052

[58] Zhang Y, Zhang H, Xu Y, Wang Y. Europium doped nanocrystalline titanium dioxide: Preparation, phase transformation and photocatalytic properties. *Journal of Materials Chemistry*. 2003;**13**:2261-2265. DOI: 10.1039/b305538h